Space Science and Engineering Center
University of Wisconsin-Madison

POSTLAUNCH STUDY REPORT
OF
VAS-H PERFORMANCE

A REPORT from the

Cooperative Institute for Meteorological Satellite Studies

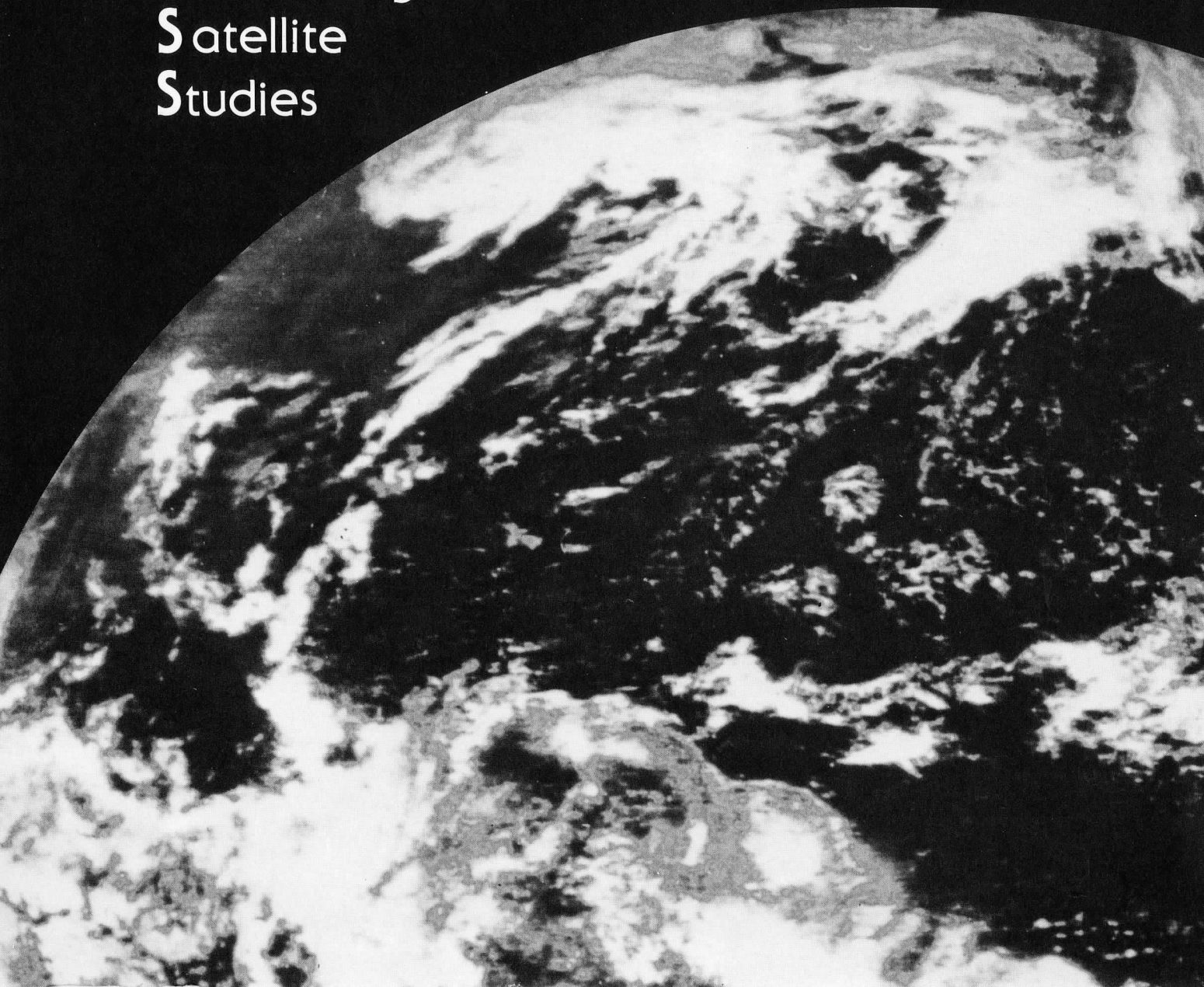

POSTLAUNCH STUDY REPORT OF VAS-H PERFORMANCE

by

Paul Menzel

Gary Wade

Advanced Satellite Products Project
NOAA/NESDIS
Madison, Wisconsin

March 1987

INTRODUCTION

The GOES-H spacecraft, carrying the VAS-H instrument, was successfully launched 26 February 1987. After some necessary station keeping maneuvers, VAS-H began transmitting engineering checkout and sounding data on 17 March. This report is based on the analyses of the inflight data. Some of the analyses of pre-launch VAS-H data are included for comparison. Many of the analyses performed for VAS-D have been repeated for VAS-H; the theoretical basis for these calculations can be found in the VAS-D pre-launch and post-launch study reports and will not be repeated here.

I. INFLIGHT VAS-F CALIBRATION

Electronic Calibration

Tables I.1 and I.2 summarize the inflight measurements of the electronic calibration waveform. The average ramp slope was found to vary between .300 and .308 volt/msec (off by up to 4% of the specified value .312 volt/msec whereas VAS-F ramp slope was within .4% of spec) and the average plateau voltage ranged from 4.45 to 4.55 volts (within 1.0% of the specified value 4.50 volts). The data confirms that the detectors are functioning properly. The observed noise level for band 9 is as high as was observed previously for VAS-F.

Radiometric Calibration

VAS radiances and forward calculations from the NMC Nested Grid Model temperatures for roughly 650 sites over the United States have been compared and the radiometric biases are found in Table I.3. VAS data from 2100 GMT on 20 March 1987 is compared to NGM 0000 GMT analysis on 21 March 1987 which has incorporated surface data from 2100 GMT on 20 March 1987. Most biases are less than 1°K. Moisture variability accounts for the differences in bands 9 and 10 and surface variability affects bands 7 and 8. However, the biases in bands 3 and 5 are much larger than previously found for VAS-F and are as yet unexplained. The bias in band 6 while large is comparable to that found for VAS-F.

Table I.1 VAS-H Electronic Calibration Ramp

filter	detector	ramp slope (volts/msec)	offset (volts)	linear regression coefficient	σ ramp (volts)
8	Upper Large HgCdTe	.305	-.742	.9999	.002
8	Lower Large HgCdTe	.306	-.719	.9999	.003
8	Upper Small HgCdTe	.306	-.753	.9999	.003
8	Lower Small HgCdTe	.303	-.716	.9999	.004
12	Upper Large InSb	.304	-.655	.9993	.042
12	Lower Large InSb	.301	-.631	.9988	.054
9	Upper Large HgCdTe	.304	-.736	.9987	.055
9	Lower Large HgCdTe	.301	-.680	.9991	.046
9	Upper Small HgCdTe	.308	-.834	.9982	.068
9	Lower Small HgCdTe	.305	-.717	.9972	.084
4	Upper Large HgCdTe	.303	-.748	.9999	.015
4	Lower Large HgCdTe	.305	-.725	.9999	.017
4	Upper Small HgCdTe	.307	-.757	.9998	.023
4	Lower Small HgCdTe	.305	-.698	.9996	.030
11	Upper Large InSb	.304	-.650	.9991	.048
11	Lower Large InSb	.300	-.638	.9986	.058

Table I.2 VAS-H Electronic Calibration Plateaus

filter	detector	zero (volts) $\bar{z}$	zero (volts) σ_z	offset (volts) $\bar{o}$	offset (volts) σ_o	plateau (volts) $\bar{p}$	plateau (volts) σ_p
8	ULH	.019	.003	.249	.002	4.506	.004
8	LLH	.026	.002	.237	.003	4.520	.003
8	USH	.009	.004	.238	.003	4.497	.004
8	LSH	.022	.003	n/a		4.481	.003
12	ULI	.007	.011	.229	.014	4.505	.019
12	LLI	.013	.018	n/a		4.457	.016
9	ULH	.056	.043	.258	.054	4.553	.050
9	LLH	.051	.040	n/a		4.503	.042
9	USH	.016	.024	.186	.061	4.443	.074
9	LSH	.076	.070	n/a		4.514	.102
4	ULH	.030	.012	.253	.011	4.486	.017
4	LLH	.042	.016	n/a		4.523	.015
4	USH	.013	.016	.257	.027	4.505	.029
4	LSH	.037	.027	n/a		4.529	.025
11	ULI	.007	.012	.226	.024	4.492	.019
11	LLI	.014	.022	n/a		4.433	.020

n/a indicates that data was not available.

Table I.3 VAS Biases with Respect to NGM Forward Calculated Radiances for Roughly 650 Sites (VAS-NGM)

band	$mW/ster/m^2/cm^{-1}$ average difference	°K difference	rms
1	.75	.80	1.62
2	-.08	-.09	.67
3	2.33	2.50	.77
4	.99	.92	.52
5	-2.54	-1.80	1.52
6	-.12	-3.56	1.00
7	-.29	-.18	2.64
8	-1.76	-1.11	2.73
9	-.80	-1.82	2.66
10	-.70	-3.00	3.24
11	n/a	n/a	n/a
12	n/a	n/a	n/a

n/a indicates that data was not available.

II. INFLIGHT VAS-F DETECTOR NOISE REDUCTION ANALYSIS

The spin budget summary of the findings during the post-launch checkout on 17 March 1987 are found in Tables II.1 and II.2. The reduced performance of the InSb detectors that was noticed in pre-launch vacuum tests is still apparent. With a spin budget of 63, the sounding rate at the subsatellite point is roughly 47.8 km/min.

The checkout revealed a low frequency (roughly 200 Hz) noise in the high gain bands (1, 2, and 9) after a filter wheel step. This is not apparent in the spin budget of Table II.1 because most of the data for these spectral bands was taken after the filter wheel had settled. Figure II.1 shows the autocovariance of the noise as a function of sampling interval τ,

$$C(\tau) = \sum_i e(t_i)e(t_i + \tau)$$

where $e(t_i)$ is the deviation of sample at t_i from the line mean, for one thousand samples of band 9 just after filter wheel movement (spin 1) and one spin later (spin 2). Normally, $C(\tau)$ is zero for uncorrelated noise, which is expected for samples 5 milliseconds apart. During spin 1, the low frequency noise is readily apparent, while it has settled out by spin 2. Subsequent spins show no further evidence of this noise.

The effect of this noise on dwell sounding is undetermined thus far. It is not thought to be very appreciable and can be filtered out by the user, if necessary. No change in satellite operation (i.e., one extra spin for bands 1, 2, and 9 to allow filter wheel settling) is anticipated. In multispectral images (see section IV), it is noticeable and will affect water vapor tracking to produce winds in band 9 (bands 1 and 2 are rarely imaged). Again, filtering by the user may be necessary.

Table II.1 Inflight Spin Budget of VAS-F Large Detectors

Band		Single Sample Noise (erg/etc) inflight	pre-launch	Spin Budget* inflight	pre-launch
1	U	5.112	5.821	2.4	3.2
	L	3.760	5.365	1.1	2.2
2	U	2.071	2.311	11.7	14.7
	L	2.010	2.697	10.5	16.1
3	U	1.340	1.347	4.6	5.1
	L	1.572	1.815	6.2	8.2
4	U	.877	.9169	2.0	2.5
	L	1.074	.9847	2.9	2.5
5	U	.964	.9574	2.4	2.5
	L	1.034	1.571	2.9	4.7
6	U	.034	.0361	13.6	14.4
	L	.035	.0353	13.7	13.8
7	U	.639	.6964	1.2	1.3
	L	.866	.9626	2.0	2.3
8	U	.098	.0736	.1	.1
	L	.032	.0802	.1	.1
9	U	.542	.5856	2.2	2.6
	L	.738	.8879	3.8	5.1
10	U	.147	.1497	.4	.4
	L	.191	.1923	.6	.6
11	U	.035	.0383	13.7	15.9
	L	.036	.0377	14.0	15.4
12	U	.009	.0093	.9	1.0
	L	.009	.0097	1.0	1.0
				61	70
				63	79

U denotes upper large detector; L denotes lower large detector.

* for sounding in 30x30 km area, except 150x150 km area for band 1.

round up for integer value of spin budget per spectral band.

Table II.2 Inflight Spin Budget of VAS-H Small Detectors

Band		Single Sample Noise (erg/etc) inflight	pre-launch	Spin Budget* inflight	pre-launch
1	U				
	L				
2	U				
	L				
3	U	2.446	2.586	16.8	17.8
	L	2.575	2.673	18.9	19.9
4	U	1.702	1.533	8.1	6.7
	L	1.686	1.707	8.3	8.4
5	U	1.684	1.667	7.8	7.8
	L	1.688	1.697	8.0	8.0
6	U				
	L				
7	U	1.387	1.378	4.9	5.1
	L	1.318	1.374	5.1	5.3
8	U	.161	.130	.1	.1
	L	.306	.147	.2	.1
9	U	1.211	1.253	10.6	11.9
	L	1.344	1.469	14.3	16.3
10	U	.309	.325	1.7	1.7
	L	.335	.336	2.1	1.9
11	U				
	L				
12	U				
	L				

U denotes upper small detector; L denotes lower small detector.

Note that bands 1, 2, 6, 11 and 12 are not available with the small detectors.

* for sounding in 15x15 km area.

round up for integer value of spin budget per spectral band.

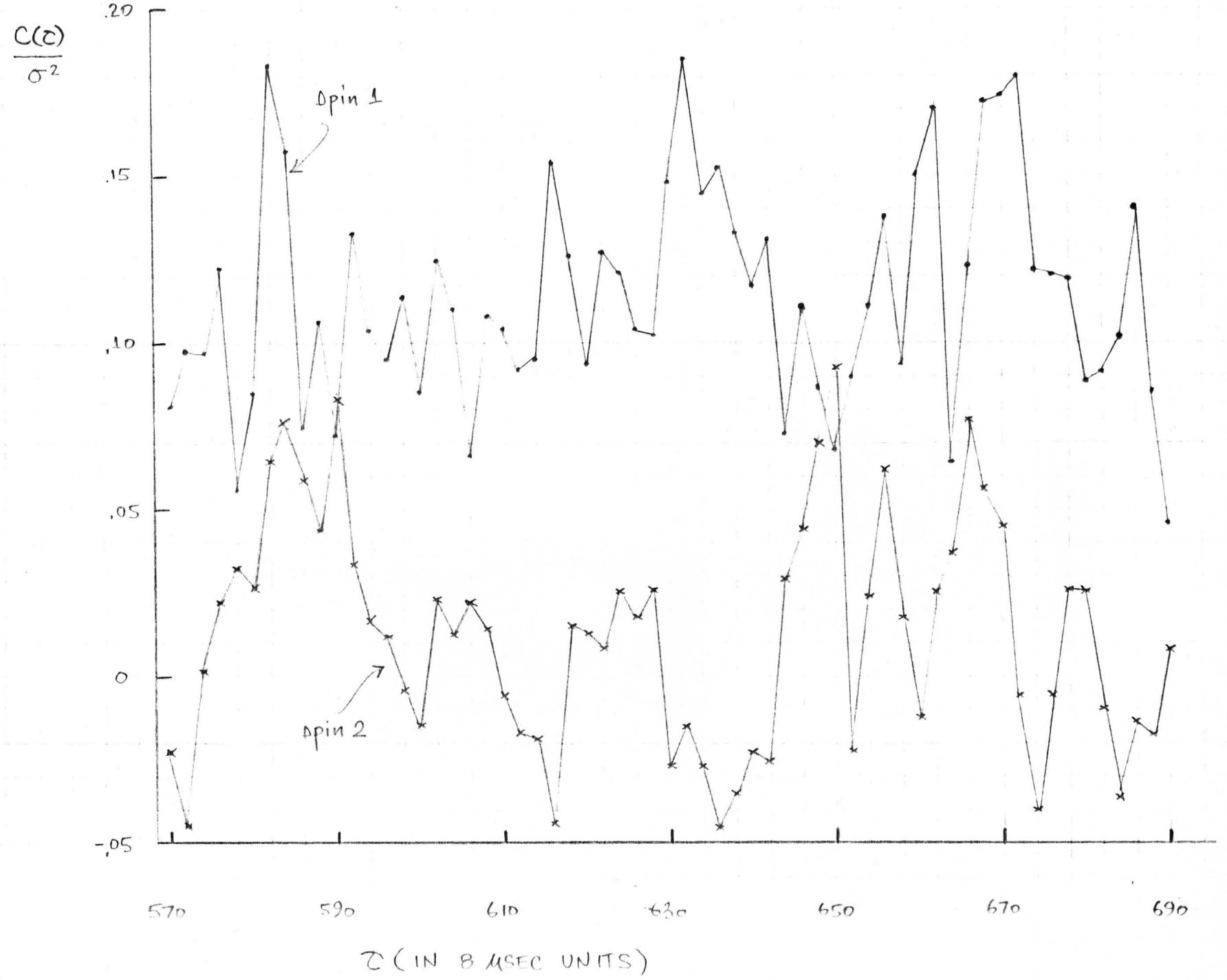
C(τ)/σ²
.20
.15
.10
.05
0
-.05
spin 1
spin 2
570
590
610
630
650
670
690
τ (IN 8 μSEC UNITS)

FIGURE II, 1

III. INFLIGHT DETERMINATION OF MISREGISTRATION OF VAS-H IMAGES

Preliminary determinations of the misregistration of images of the IR window channels (band 8 using HgCdTe detectors, band 12 using InSb detectors) and the visible channel were made from 17 March 1987 images. It was found that the large detector IR images are east of the visible image, while the small detector IR images line up somewhat west of the visible image. The IR images of all detectors appear south of the visible image. Table III.1 summarizes these findings. Corrections for the EW displacement will be made in the VIP. The cause for these misalignments is not understood.

Table III.1 Misregistration of VAS-H Images

East West

B / A	Visible	HgCdT(L)	HgCdTe(S)	InSb
Visible	-	.40	-.29	.15
HgCdTe(L)	-.40	-	-.69	-.25
HgCdTe(S)	.29	.69	-	.44
InSb	-.15	.25	-.44	-

Image A is X milliradians west of Image B

North South

B / A	Visible	HgCdT(L)	HgCdTe(S)	InSb
Visible	-	.11	.11	.13
HgCdTe(L)	-.11	-	0	.02
HgCdTe(S)	-.11	0	-	.02
InSb	-.13	-.02	-.02	-

Image A is X milliradians north of Image B

IV. VAS-H MULTISPECTRAL IMAGES

The following figures show the multispectral images of the twelve VAS-H spectral bands that were generated during the post-launch checkout. Bands 1, 2, and 9 exhibit the low frequency noise occurring during filter wheel stepping. Amplitude of the noise is roughly 20% of the range of values within the image, which translates into approximtaely 250 mV.

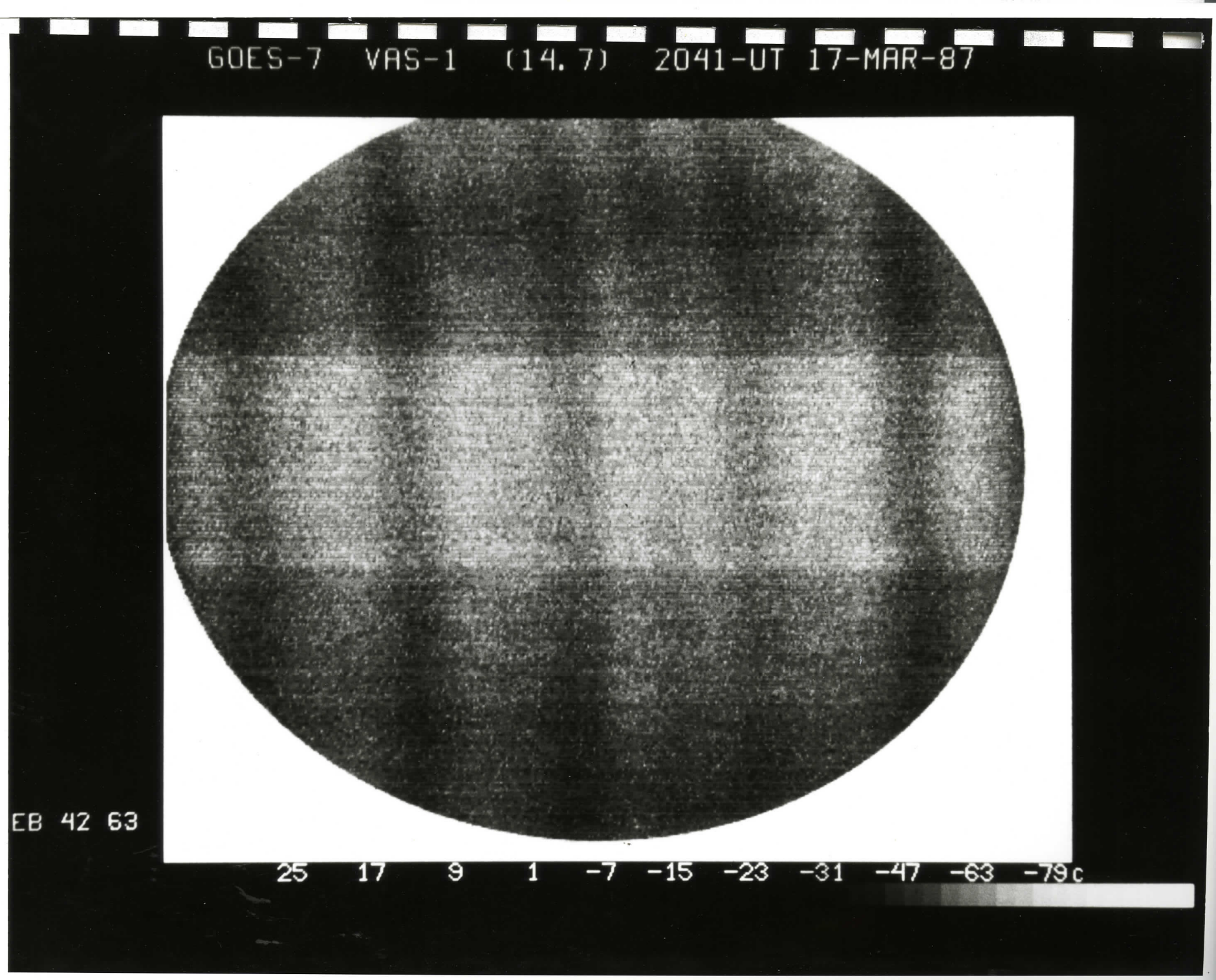
GOES-7 VAS-1 (14.7) 2041-UT 17-MAR-87
EB 42 63
25 17 9 1 -7 -15 -23 -31 -47 -63 -79c

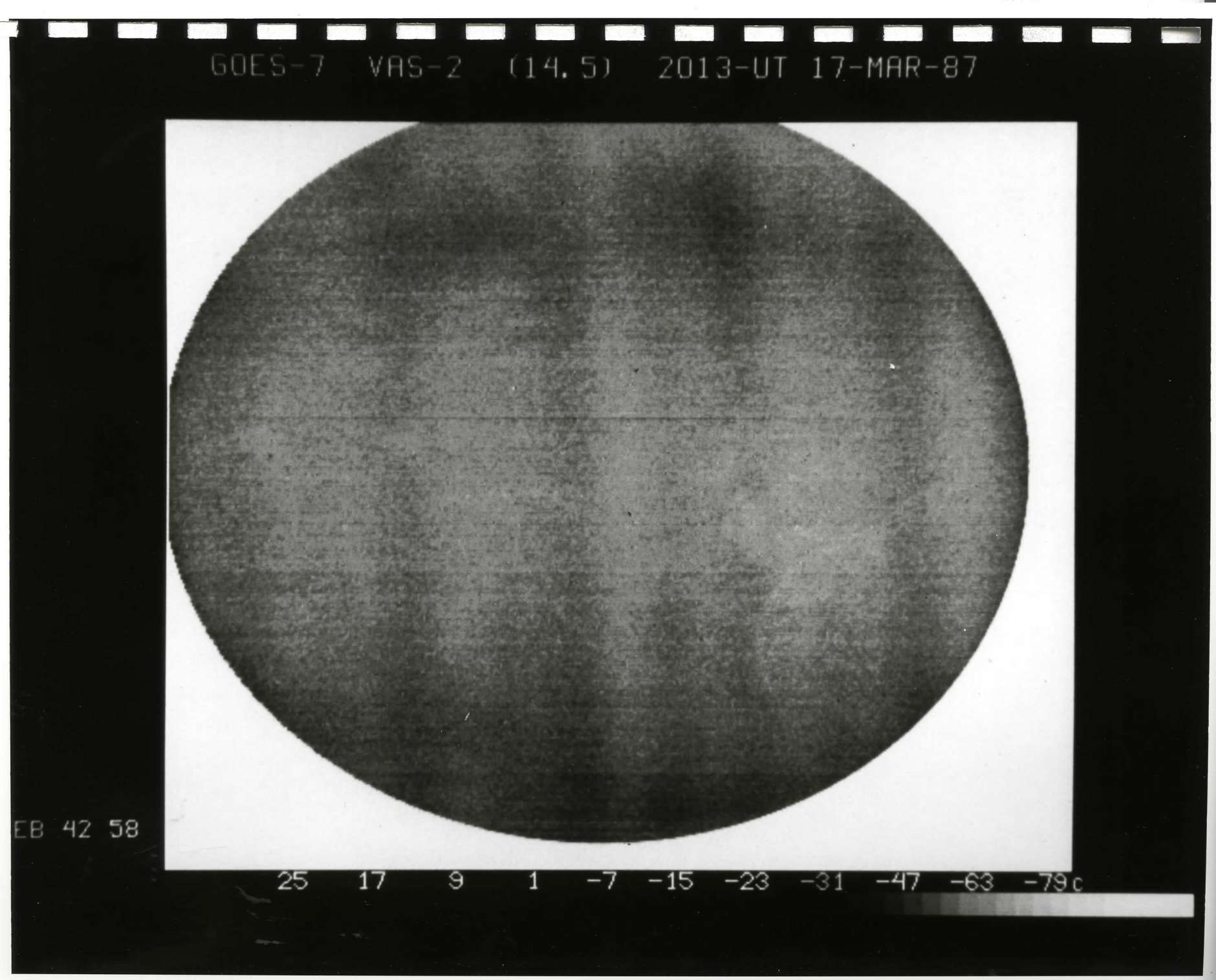
GOES-7 VAS-2 (14.5) 2013-UT 17-MAR-87
EB 42 58
25 17 9 1 -7 -15 -23 -31 -47 -63 -79 C

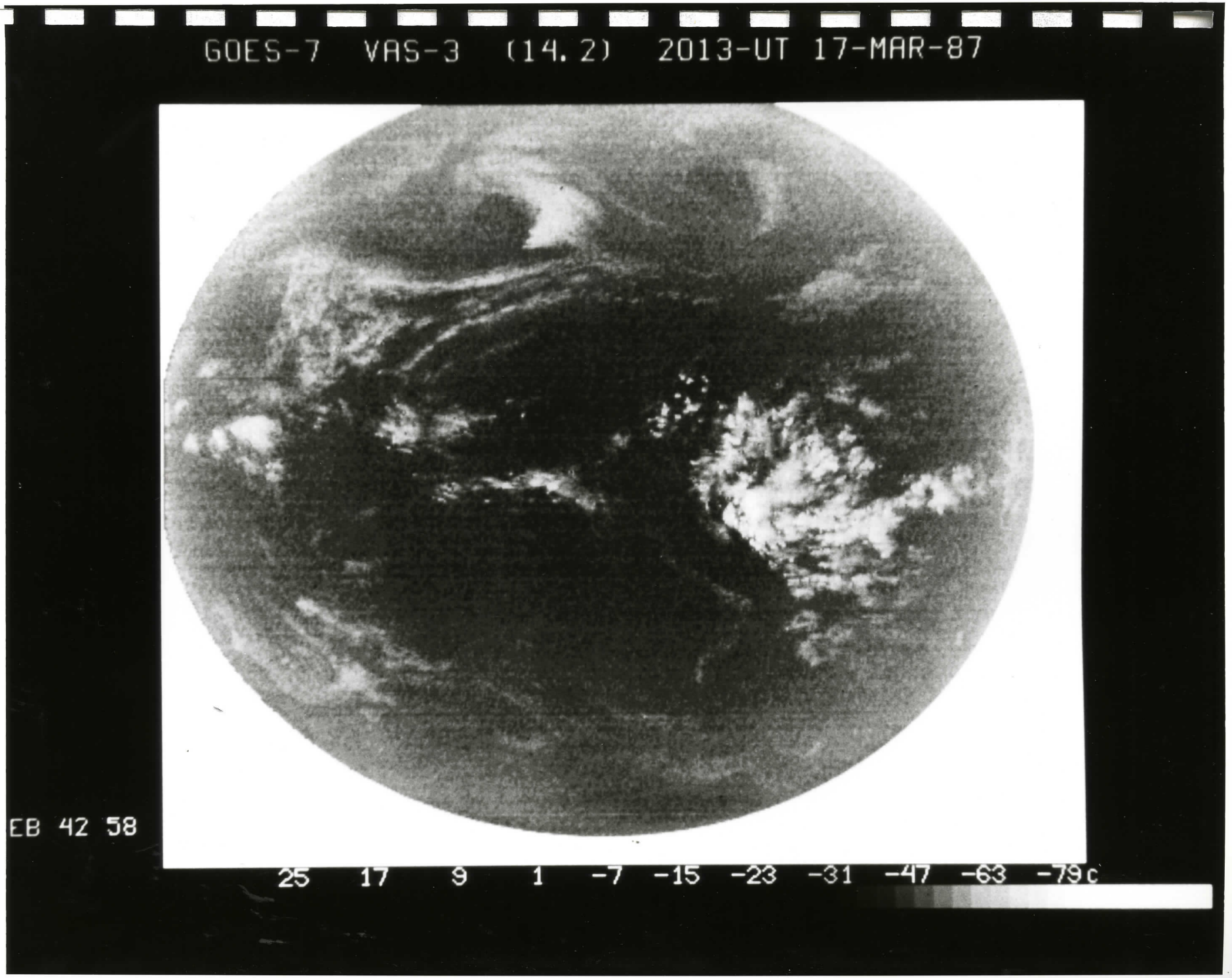
GOES-7 VAS-3 (14.2) 2013-UT 17-MAR-87
EB 42 58
25 17 9 1 -7 -15 -23 -31 -47 -63 -79c

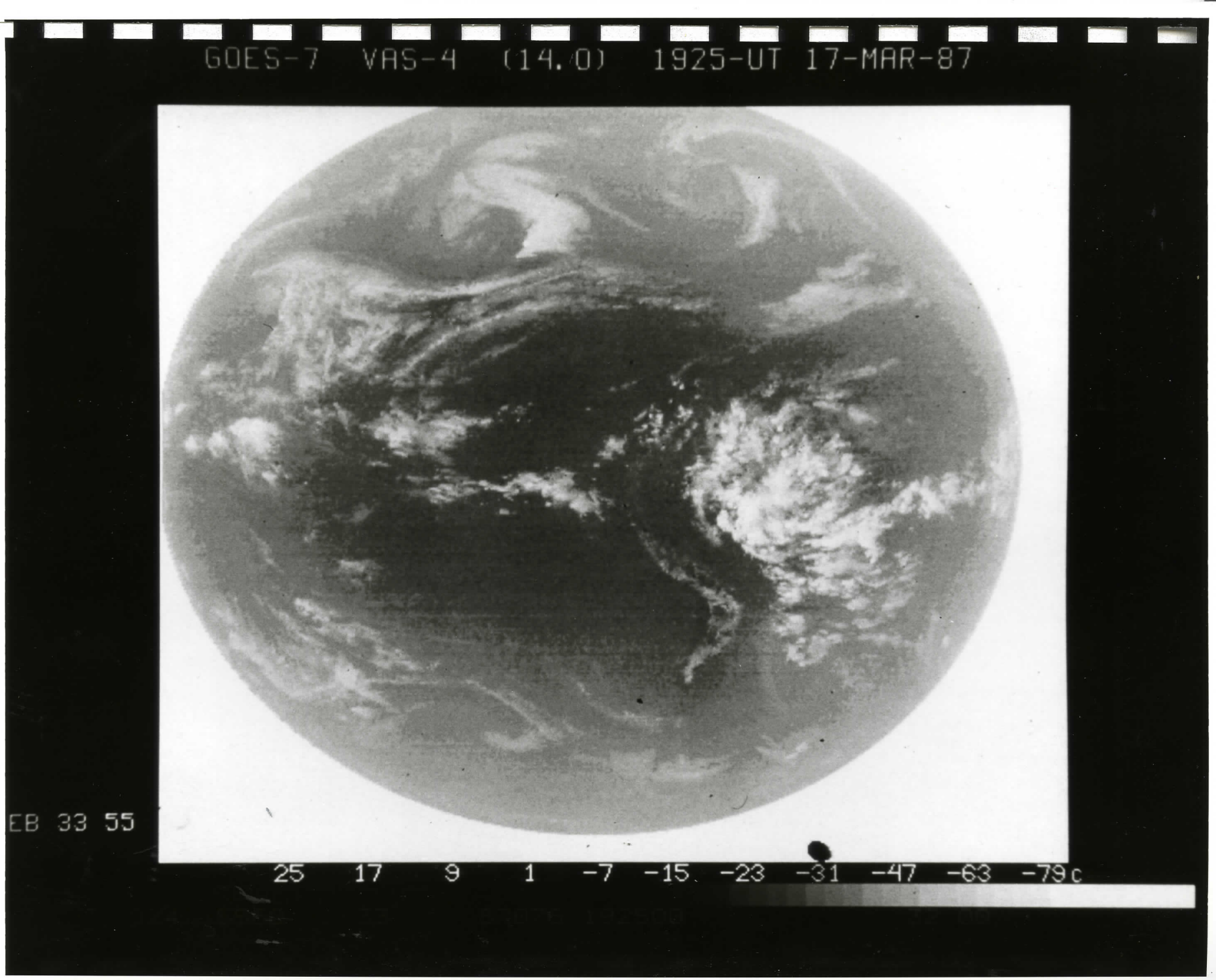
GOES-7 VAS-4 (14.0) 1925-UT 17-MAR-87
EB 33 55
25 17 9 1 -7 -15 -23 -31 -47 -63 -79c

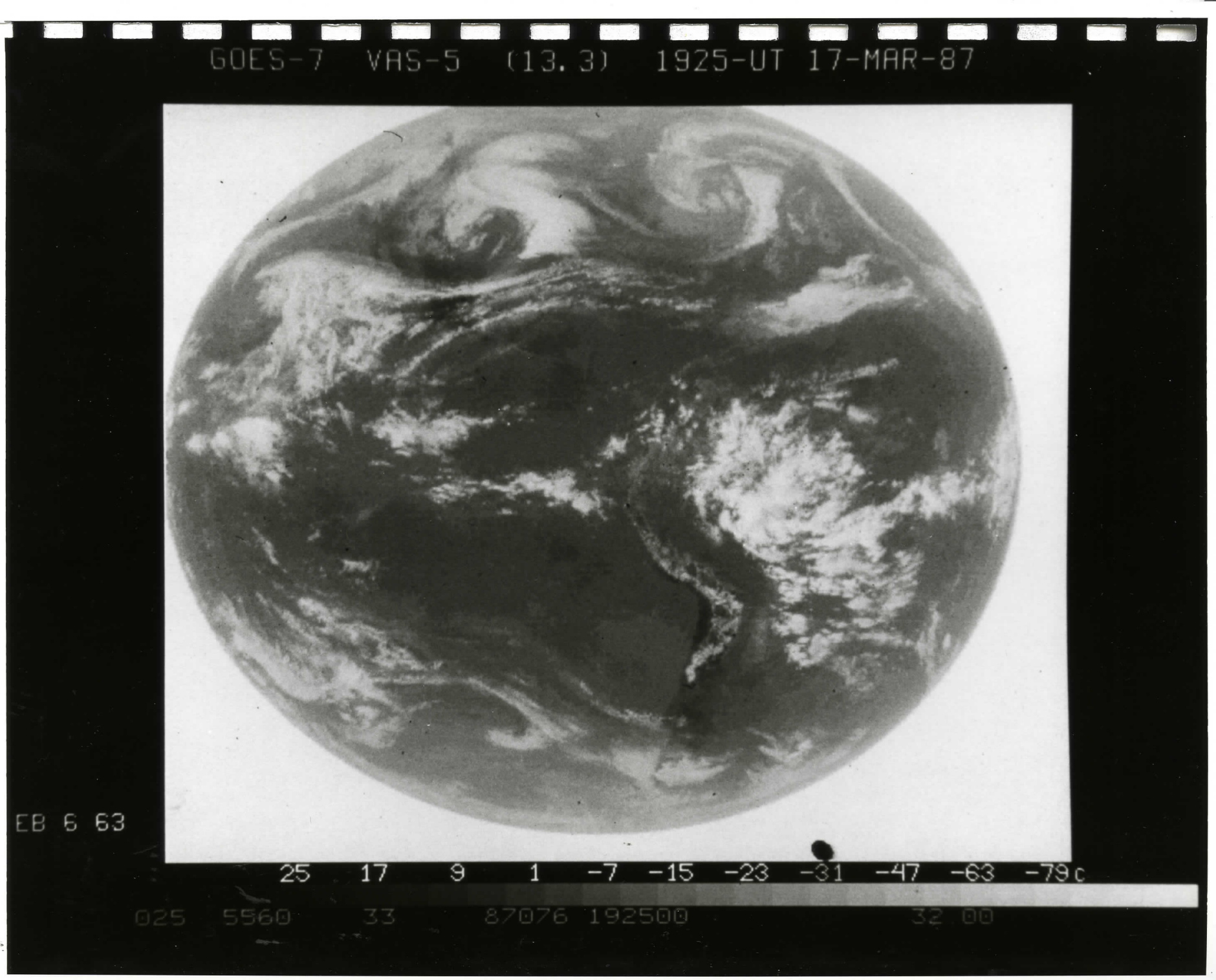
GOES-7 VAS-5 (13.3) 1925-UT 17-MAR-87
EB 6 63
25 17 9 1 -7 -15 -23 -31 -47 -63 -79c
025 5560 33 87076 192500 32 00

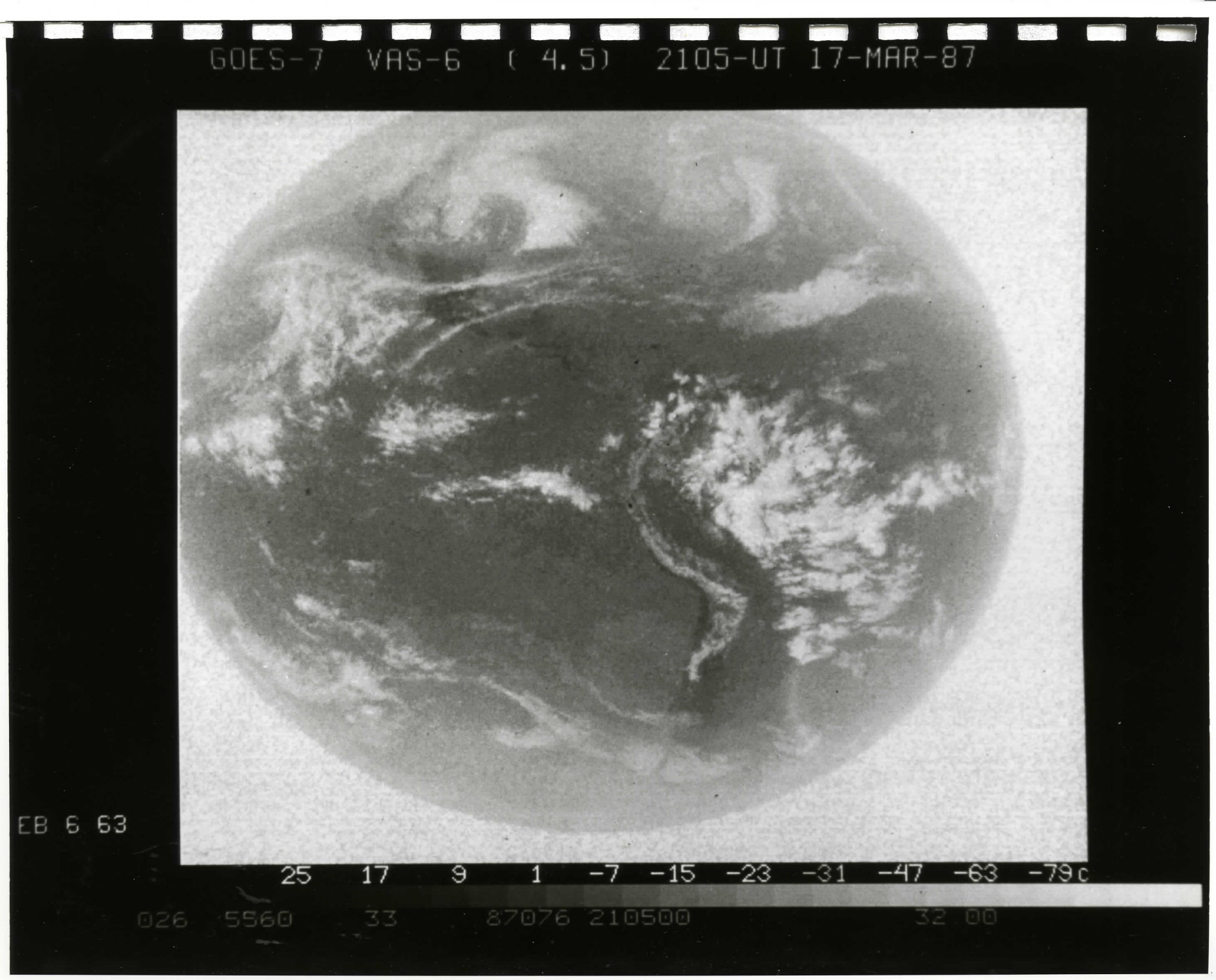
GOES-7 VAS-6 (4.5) 2105-UT 17-MAR-87
EB 6 63
25 17 9 1 -7 -15 -23 -31 -47 -63 -79c
026 5560 33 87076 210500 32 00

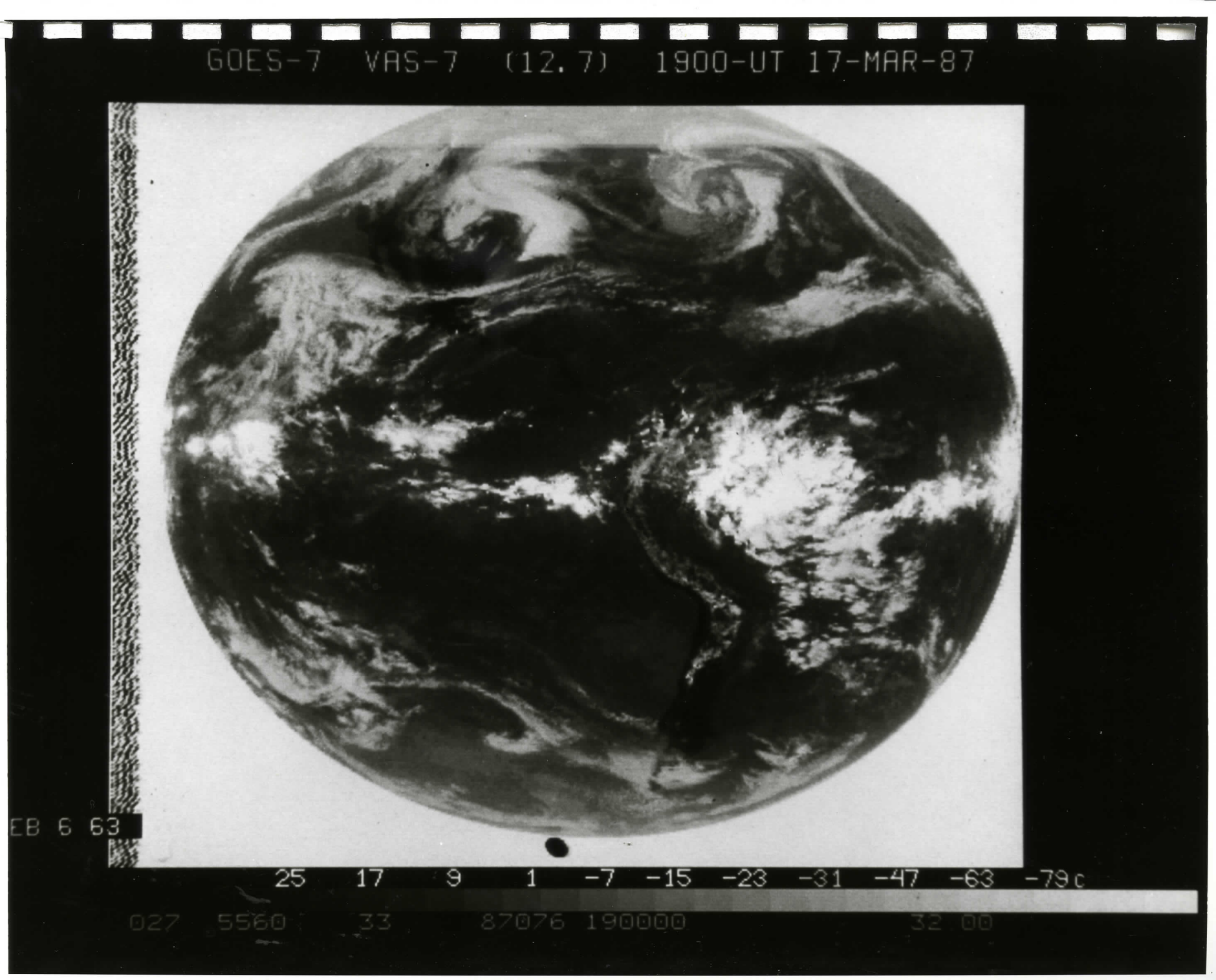
GOES-7 VAS-7 (12.7) 1900-UT 17-MAR-87
EB 6 63
25 17 9 1 -7 -15 -23 -31 -47 -63 -79c
027 5560 33 87076 190000 32 00

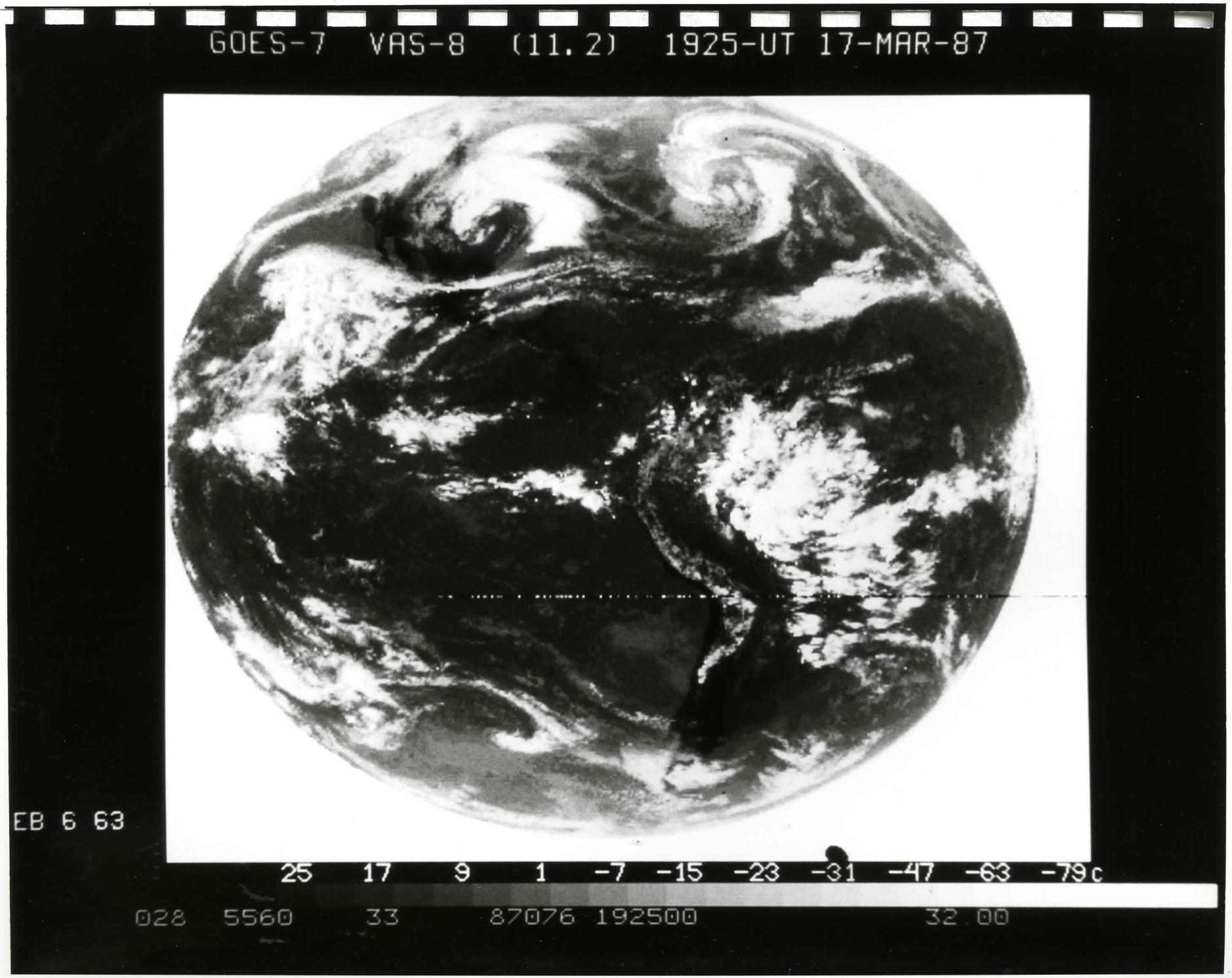
GOES-7 VAS-8 (11.2) 1925-UT 17-MAR-87
EB 6 63
25 17 9 1 -7 -15 -23 -31 -47 -63 -79c
028 5560 33 87076 192500 32 00

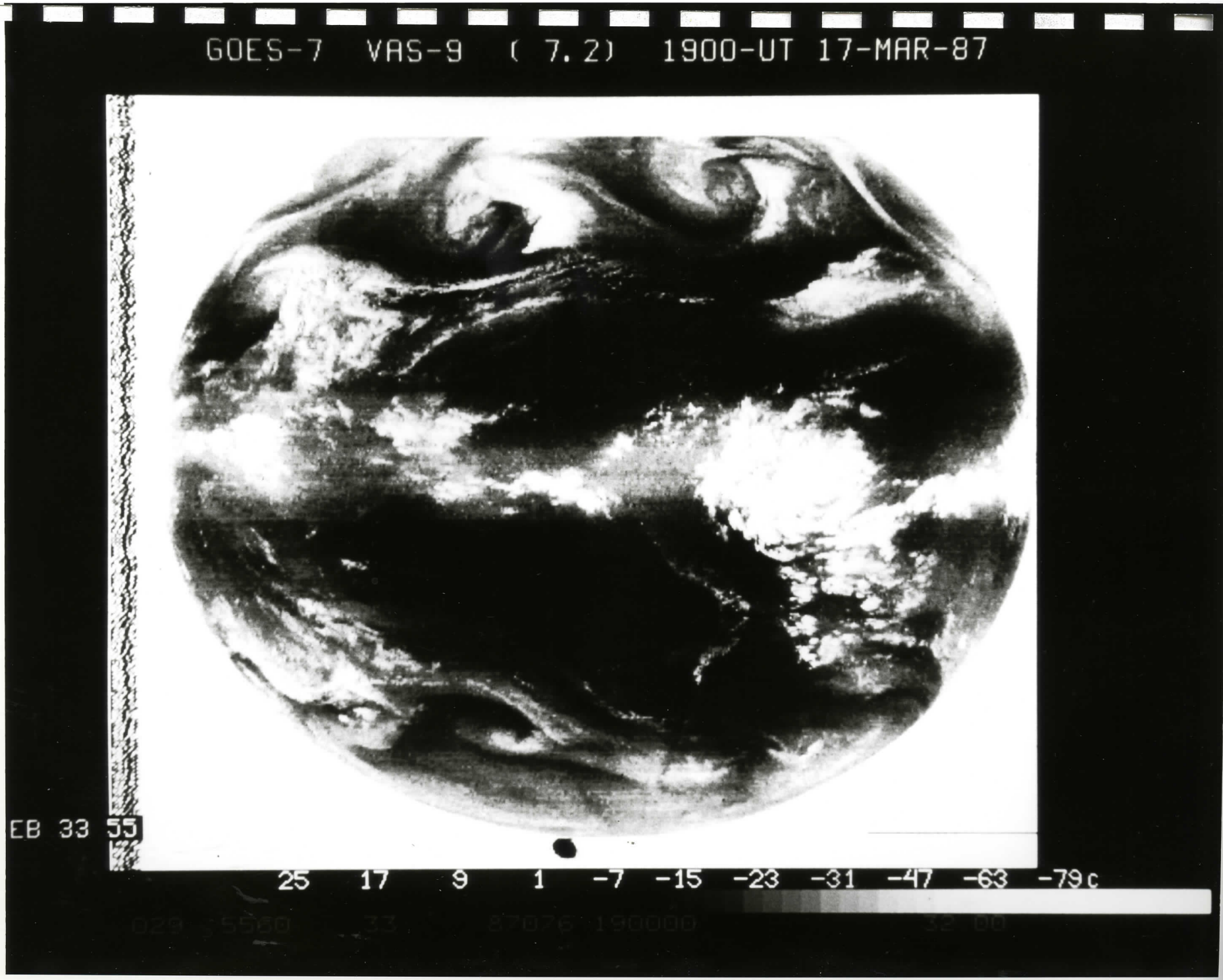
GOES-7 VAS-9 (7.2) 1900-UT 17-MAR-87
EB 33 55
25 17 9 1 -7 -15 -23 -31 -47 -63 -79c

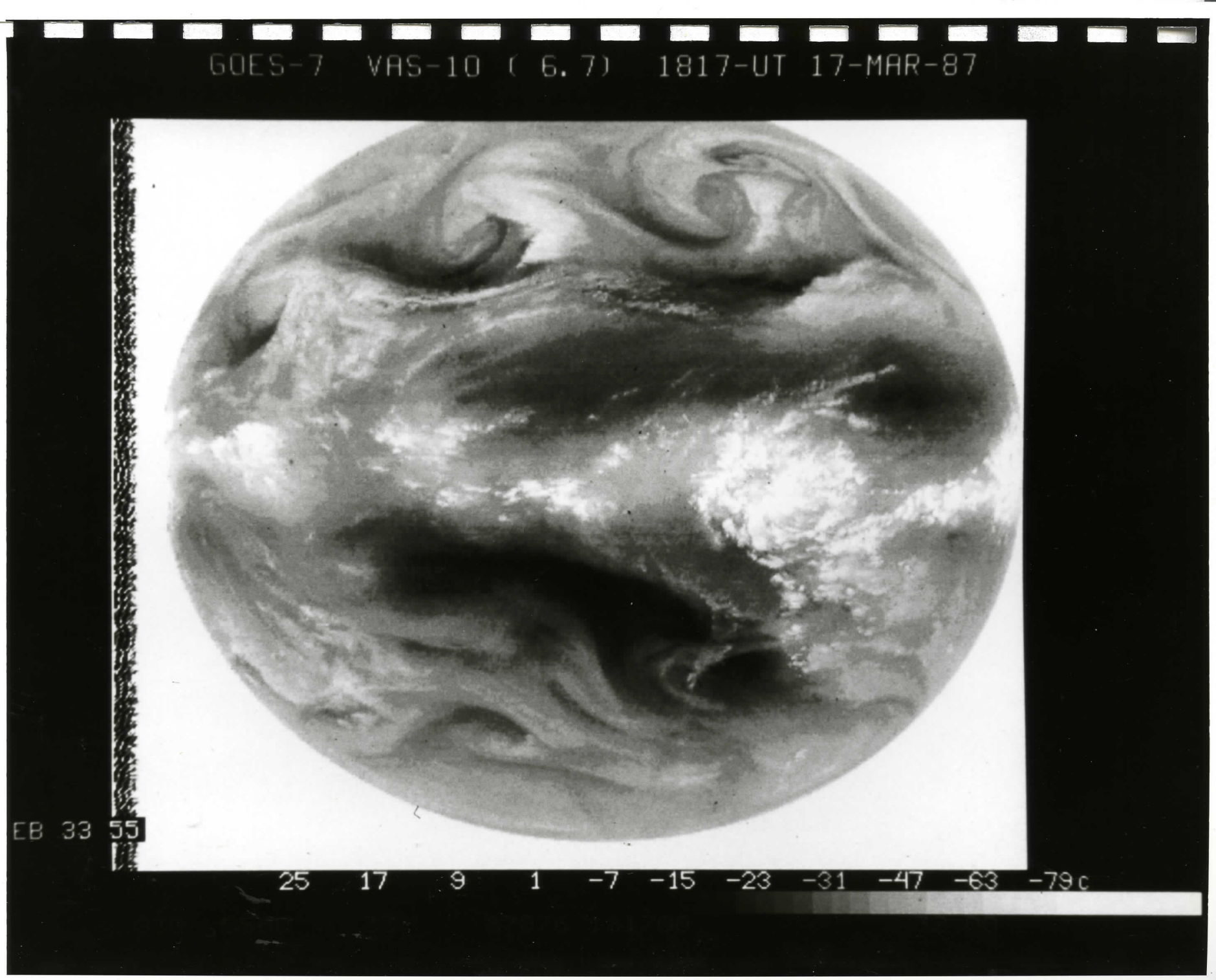
GOES-7 VAS-10 (6.7) 1817-UT 17-MAR-87
EB 33 55
25 17 9 1 -7 -15 -23 -31 -47 -63 -79c

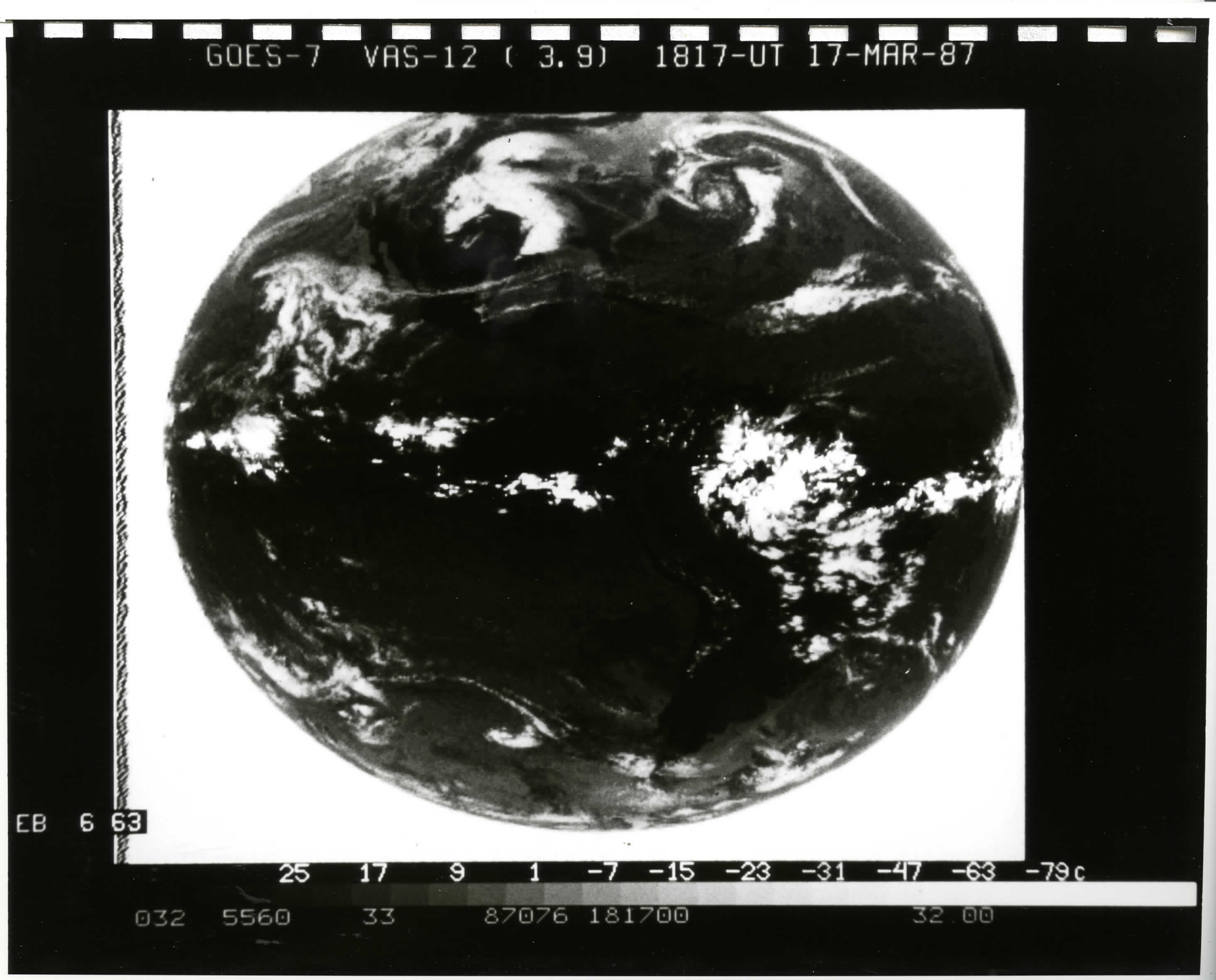
GOES-7 VAS-12 (3.9) 1817-UT 17-MAR-87
EB 6 63
25 17 9 1 -7 -15 -23 -31 -47 -63 -79c
032 5560 33 87076 181700 32 00